UDC 532.528

THEORETICAL AND EXPERIMENTAL STUDY OF DYNAMICS OF SUPERCAVITATING VEHICLES WITH CONE CAVITATORS

V. V. Moroz[1†], V. O. Kochin[1], V. M. Semenenko[1], Bu-Geun Paik[2]

[1] *1Institute of Hydromechanics of NAS of Ukraine*
Marii Kapnist Str., 8/4, 03057, Kyiv, Ukraine
[†] *E-mail: MorozVV@nas.gov.ua*

[2] *Korea Research Institute of Ships & Ocean Engineering*
32, Yuseong-daero 1312 beon-gil, Yuseong-gu, Daejeon, 34103, Republic of Korea

Received 22.02.2021 ◇ Revised 30.04.2024

A mathematical model of a supercavitating underwater vehicle dynamics based on the complete set of equations of the 6-DOF motion of an elongated solid body is considered. Originating from the G. V. Logvinovich's principle of independence of the cavity section expansion, the approximation mathematical model of a 'slender' cavity is used to calculate the supercavitation flow. The hydrodynamic forces acting on various structural elements of the underwater vehicle were estimated using the approximation dependencies obtained both from the experiments, and the theoretical solutions. The developed mathematical model of the supercavitating vehicle dynamics has been verified by comparing the calculated parameters with those obtained during towing tests of the model of a supercavitating underwater vehicle in the high-speed experimental tank at the Institute of Hydromechanics of the National Academy of Sciences of Ukraine. The main attention was paid to the dynamics of supercaviting models with the cone cavitators. Basing on the experimental results, the new approximation formula for the lift on the inclined cone cavitators was proposed. The simulated and the experimental shapes of the stationary and non-stationary cavities behind the inclined cone cavitators were compared. Verification of the mathematical model 'as a whole' was carried out by comparing the calculated kinematic parameters with those obtained during the towing tests of the movable supercavitating model with one degree of freedom in pitch. Various modes of the motion of the supercavitating model were organized in the tests: planing along the lower cavity's wall; planing along the upper cavity's wall; motion with the fins without touching the cavity walls by the model body; oscillatory motion between the upper and lower cavity walls. The experimental and calculated kinematic characteristics of the supercavitating model are compared. Their sufficiently good qualitative and quantitative agreement shows that the developed mathematical model adequately predicts the dynamic behavior of the underwater supercavitating vehicle.

KEY WORDS: supercavitating vehicle dynamics, cone cavitator, mathematical model, computer simulation, experimental verification

NOMENCLATURE

c_x	the drag coefficient;
c_y	the lift coefficient;
c_y^δ	the derivative of the lift coefficient with respect to the inclination angle;
D_n	the cone cavitator base diameter;
D_c	the cavity mid-section diameter;
F	the force;
Fr	the Froude number, $\mathrm{Fr} = V/\sqrt{gD_n}$;
g	the gravity acceleration;
H	the immersion depth;
h_f, h_g	the cavity axis deformations;
L_c	the cavity length;
p_c	the cavity pressure;
p_w	the water pressure;
q	the velocity head, $q = \rho V^2/2$;
Q_V	the volumetric air rate;
S	the cavity cross-section area;
S_n	the cone cavitator base area, $S_n = \pi D_n^2/4$;
V	the velocity;
x, y, z	the coordinates of the model mass center.

Greek Symbols

β_n	the cone cavitator angle, $\beta_n = 2\gamma$;
γ	the cone cavitator half-angle;
δ_{fh}, δ_{fv}	the angles of fin deflection;
δ_z	the angle of cavitator inclination;
ρ	the water density;
σ	the cavitation number, $\sigma = 2(p_w - p_c)/(\rho V^2)$;
ψ	the model pitch angle.

1. INTRODUCTION

Supercavitation is one of the promising ways to create high-speed underwater vehicles [1, 2]. When moving in supercavitation regime, a special nose cavitator creates a cavity filled with water vapor or gas around the vehicle body. In this case, the hydrodynamic drag of the vehicle falls dramatically. The disk cavitators are the most widely used. However, nowadays, cavitators of other shapes, in particular, conical, have started to be actively used. In this case, a cavitator is considered not only for creating a cavity, but also as operating control of this vehicle motion.

From the early stages of designing underwater supercavitating vehicles (SC-vehicles), it is necessary to estimate their dynamic properties. For this purpose, mathematical models of dynamics with various degrees of complexity are used. Mathematical models of the underwater SC-vehicle dynamics contain interrelated differential equations of dynamics of the underwater vehicle as a rigid body, equations of dynamics of an unsteady cavity, and equations for the hydrodynamic forces and moments acting on the underwater vehicle.

The approximation mathematical model of a 'slender' cavity based on the G. V. Logvinovich's principle of independence of the cavity section expansion [1] is most often used to calculate the parameters of unsteady supercavitation flow around an underwater vehicle. To determine the hydrodynamic forces acting on various structural elements of the underwater vehicle (cavitator, body, fins), various approximation dependences obtained based on both the experimental data and the theoretical studies are used [3,4]. This of mathematical model naturally demonstrates such features of unsteady supercavitation flows as 'cavity memory', delayed cavity response to perturbations, and discontinuous hydrodynamic characteristics.

As a result, the 'fast' computational algorithms have been developed at the Institute of Hydromechanics of the National Academy of Sciences of Ukraine (IHM NASU), which made it possible to observe the dynamic behavior of supercavitating models (SC-models) on a computer screen directly during the calculation [5]. With the use of computer simulation, various problems were investigated: the problem of the SC-vehicle speeding-up [6, 7], comparative analysis of different ways of control the SC-vehicle motion [8, 9], the possibility of the SC-vehicle maneuvering on depth and course [10, 11], loss of stability and self-induced oscillation of the ventilated cavities [12], etc.

Some components of the G. V. Logvinovich's theory were used in many works to study the dynamics and control of SC-vehicles with varying degrees of completeness (see, for example, [13–15].

In practice, nose cavitators are used not only for creating the cavity but also for controlling the SC-vehicle motion. In this case, the lateral force required for control arises when the cavitator is inclined relative to the incoming flow. Up to the present, the expression for the lateral force on an inclined disk cavitator obtained by G. V. Logvinovich has been successfully used [1]. Many works are devoted to the experimental study of supercavitation flows over axisymmetric cone cavitators [16, 17]. However, the lateral forces on the inclined cone cavitators were investigated still not enough [18]. It was found that the dependence of the lateral force on the inclination angle for the 'blunt' cone cavitators $\beta_n > 90°$ is quite similar to that for a disk cavitator. However, this is not true for 'non-blunt' cone cavitators $\beta_n < 90°$. The absence of such a dependence made it impossible to study theoretically the dynamics of SC-models with the 'non-blunt' cone cavitators.

Formulae for the planing forces of a body within a cavity were obtained theoretically by applying both Wagner's theory and the principle of the plane sections [4, 19, 20]. Paryshev's formulae (or similar ones) are used in almost all works devoted to the SC-model dynamics (see, for example, [8, 13, 21]. Therefore, their experimental verification is a crucial task and has been carried out repeatedly [22–25].

As shown in the works [11, 26], the ability to maneuver of vehicles using only a cavitator is limited. Therefore, in practice, the hydrodynamic cavity-piercing fins are used for the control of the SC-vehicle motion. In this case, several features complicate their use and reduce their efficiency [10]. The results of experimental studies of the forces on the cavity-piercing fins are presented, for example, in papers [27–29].

The key point in constructing and practically using computational algorithms is the reliability of the approximation mathematical models and dependences. Verification of the mathematical model reliability is done by comparing the calculated data with the results of a model experiment.

Typically, model experiments are carried out in the inverted flow of hydrodynamic tun-

nels. In this case, the tested model is mounted motionlessly on a multicomponent dynamometer, and the direction of the incoming flow is changed by rotating hydrodynamic wings, which are installed in front of the model [30], or a rotary cavitator [31]. This kind of research is well suited for checking the correctness of the determination of the hydrodynamic forces acting on the vehicle's structural elements. But for direct verification of the reliability of the mathematical model of the underwater vehicle dynamics 'as a whole', it is necessary to carry out experiments in which the model can move freely in space under the action of hydrodynamic forces. Such studies have not yet been carried out due to big technical difficulties.

The purpose of this paper is to check experimentally the developed mathematical model of dynamics of the underwater SC-vehicle with cone cavitators 'as a whole' and its components. The main relationships of the tested mathematical model are given in Section 2. A description of the experimental unit and the test procedure is given in Section 3, which also provides experimental data for the lateral force on the inclined cone cavitators. As a result, the approximation formula is proposed for the derivative of this force with respect to the cavitator inclination angle. In Section 4, a comparison between theoretical and experimental cavity shapes behind disk and cone cavitators is given. Section 5 presents the results of experimental studies of the SC-model dynamics. The verification of the mathematical model 'as a whole' was carried out by comparing the calculated kinematic parameters with similar parameters obtained during towing tests of the SC-model. In this case, the movable models with disk and cone cavitators and fins were tested, having one degree of freedom in pitch.

2. MATHEMATICAL MODEL

Computer simulation of the underwater SC-vehicle motion is performed by the numerical integration of the set of equations which include:

1) the known differential equations of an axisymmetric rigid body 6-DOF dynamics (see, for example, [8];

2) the equations to calculate an unsteady cavity shape and position;

3) the equations connecting hydrodynamic forces and moments acting on a SC-vehicle with the cavity and vehicle motion parameters.

2.1. Cavity shape

The following assumptions are accepted for the cavity calculation:

- the cavitation number σ is sufficiently small, and the Froude number Fr is sufficiently great;
- the slender body theory is used when calculating the hydrodynamic forces at the interaction between the model and the cavity walls;
- the cavity separation line is fixed during motion;
- cross-sections of the unsteady cavity maintain a circular shape during motion;
- a time dependence of all acting forces is quasi-stationary.

2.1.1. Steady cavity past a disk

The G. V. Logvinovich's formula of a composite cavity [1,32] is used to calculate the steady axisymmetric cavity shape. In this case, the cavity frontal part shape and the cavity basic part shape are calculated by formulae:

$$S(x) = S_n\left(1 + \frac{3x}{R_n}\right)^{2/3}, \qquad x \le x_1, \tag{1}$$

$$S(x) = S_1 + k_1\frac{x - x_1}{2}\left(R_n A\sqrt{c_{x0}} - \sigma_0\frac{x - x_1}{2}\right), \qquad x_1 < x \le L_c, \tag{2}$$

where S is the cavity cross-section area; R_n is the cavitator radius; $S_n = \pi R_n^2$ is the cavitator area; $S_1 = S(x_1)$ is the area of the 'agreement section' of the frontal part and the basic part of the cavity; $k_1 = 4\pi/A^2$; $A \approx 2$ is the empirical constant. The frontal part length is accepted $x_1 = D_n$ for the best agreement with the experimental data.

The approximation formulae are used to determine the cavity axis deformation under the action of both the transversal force on the cavitator and the gravity effect [33]:

$$h_f(x) = -c_y R_n\left(0.46 - \sigma + \frac{\bar{x}}{2}\right), \qquad c_y = \frac{F_{ny}}{qS_n}, \tag{3}$$

$$\bar{h}_g(x) = \frac{(1+\sigma)\bar{x}^2}{3Fr_l^2}, \qquad \mathrm{Fr}_l = \frac{V_\infty}{\sqrt{gL_c}}, \tag{4}$$

where $\bar{x} = x/L_c$; $\bar{h}_g = h_g/L_c$; $q = \rho V^2/2$ is the velocity head. Formula (3) is well matched with experimental data for $0.02 \le \sigma \le 0.1$. Formula (4) well corresponds with the experiment for $0.05 \le \sigma \le 0.1$, $2.0 \le Fr_l \le 3.5$.

2.1.2. Steady cavity past a cone

To calculate the shape of the cavity past a cone cavitator, the method of the equivalent disk cavitator is used [34]. The equivalent disk is a cavitator with the same cavitation drag, its diameter is equal to:

$$D_n^{(eq)} = \frac{D_n}{\varepsilon}, \qquad \varepsilon = \sqrt{\frac{0.8275}{c_{x0}(\gamma)}} \ge 1, \tag{5}$$

where D_n is the cone base diameter; γ is the cone cavitator half-angle; $c_{x0}(\gamma)$ is the cavitation drag coefficient for a cone when $\sigma = 0$ (see below (16)). Then, for the same cavitation number, the cavity past the cone and its equivalent disk will have the same dimensions:

$$D_c = D_n\sqrt{\frac{c_{x0}(1+\sigma)}{\kappa\sigma}} = D_n^{(ef)}\sqrt{\frac{0.8275(1+\sigma)}{\kappa\sigma}}, \qquad L_c = D_n\frac{A\sqrt{c_{x0}}}{\sigma} = D_n^{(ef)}\frac{A\sqrt{0.8275}}{\sigma}, \tag{6}$$

where $\kappa = (0.9\ldots1.0)$ and $A \approx 2$ are the empirical constants. Thus, the calculation of the cavity past the cone cavitator is replaced by the calculation of the cavity past the equivalent disk cavitator.

We use formulae (1), (2) when $\gamma > 45°$. In the case $20° \le \gamma \le 45°$, the following approximation formula is proposed instead (1):

$$S(x) = S_n \left(1 + \operatorname{tg}\gamma \frac{3x}{R_n}\right)^{2/3}, \qquad x \le x_1. \tag{7}$$

Formula (3) for the cone cavitators is transformed to the form:

$$h_f(x) = -\varepsilon c_y R_n (0.46 - \sigma + 2\bar{x}). \tag{8}$$

Formula (4) does not change in the case of the cone cavitators.

2.1.3. Unsteady cavity

The G. V. Logvinovich's principle of independence of the cavity section expansion [35, 36] is the basis of the method for calculating the unsteady cavity shape in this mathematical model. It predicates that the expansion of each cavity cross-section occurs independently of the previous and next motion of the cavitator, and it is defined by the cavitator velocity at the instant of this section formation and by the pressure variation in the ambient flow and in the cavity. The expression for the axisymmetric ventilated cavity section area on the basic cavity part is as follows [32, 35]:

$$S(\tau, t) = \pi R_1^2 + \frac{k_1}{4} A D_n V(\tau) \sqrt{c_{x0}} (t - \tau) - \frac{k_1}{2} \int_\tau^t (t - s)\sigma(\tau, s) ds, \tag{9}$$

where $\tau \le t$ is the instant of the cavitator transition through the section $0 < \xi < L_c$. The cavitator velocity $V(\tau)$ when forming the section ξ is determined from a solution of the problem of the SC-model dynamics. Following the independence principle at each instant in the fixed coordinates the coordinates of contours of axial cavity sections are determined by relations:

$$y_{cav}(\tau, t) = \pm R(\tau, t) + y_n(\tau) + h_{fy}(\tau, t) + h_{gy}(\tau, t), \tag{10}$$

$$z_{cav}(\tau, t) = \pm R(\tau, t) + z_n(\tau) + h_{fz}(\tau, t), \tag{11}$$

where $R = \sqrt{S/\pi}$ is the radius of the current cavity cross-section. Coordinates of the cavitator center path (x_n, y_n, z_n) are equal to:

$$\begin{aligned} x_n(t) &= x(t) + x_c \cos\psi(t) \cos\phi(t), \\ y_n(t) &= y(t) + x_c \sin\psi(t) \cos\phi(t), \\ z_n(t) &= z(t) - x_c \sin\phi(t). \end{aligned} \tag{12}$$

Here (x_n, y_n, z_n) are the current coordinates of the model mass center; x_c is the distance from the cavitator to the model mass center. The cavity axis distortion h_{fy}, h_{fz}, h_{gy} under the action of both the lateral force on the inclined cavitator and gravity are approximately taken into account by formulae (3), (4).

Equation of the mass of the gas in the cavity balance and relations for the gas loss from the cavity are added to this mathematical model in the case of ventilated cavities [37]. It makes it possible to perform computer simulation of such unsteady processes as loss of stability and self-induced oscillation of the ventilated cavities [12] and the cavity control by regulating the gas-supply into the cavity [6, 7].

2.2. Forces

2.2.1. Forces on a disk cavtator

In the case of the disk cavitators the known Reichardt formula is valid:

$$c_x(\sigma) = c_{x0}(1+\sigma), \qquad 0 < \sigma < 1.2, \tag{13}$$

where c_{x0} is the cavity drag coefficient when $\sigma = 0$. The numerical calculation gives value $c_{x0} = 0.8275$ [3].

In the case of the inclined disk cavitator the force is directed oppositely to the normal $\vec{n}$ to the cavitator plane: $\vec{F}_n = -F_n\vec{n}$. If the normal to the cavitator is inclined to the flow on the angle δ, then the absolute value of the force is equal to [1]:

$$F_n = \left|\vec{F}_n\right| = F_{x0}\cos\delta, \qquad F_{x0} = c_{x0}qS_n. \tag{14}$$

Relation for projections of the vector $\vec{F}_n$ in both the body and the flow coordinates, see in [8].

2.2.2. Forces on a cone cavitator

The axisymmetric cone cavitator drag F_{nx} consists of two parts: the cavitation drag F_{nx1}, and the viscous friction drag F_{nx2}:

$$F_{nx} = F_{nx1} + F_{nx2} = qS_n\left(c_{x1} + \frac{c_f}{\sin\gamma}\right), \tag{15}$$

where $c_f(\mathrm{Re})$ is the viscous drag coefficient; Re is the Reynolds number with respect to the cone generatrix. The viscous drag coefficient for the cone is calculated by the formula for the turbulent boundary layer [38]. Values of the coefficient $c_{x1}(\gamma, \sigma)$ are calculated by approximation of the numerical calculation results [3]:

$$c_{x1} = 0.5 + 1.81(\gamma/180 - 0.25) - 2.0(\gamma/180 - 0.25)^2 + (0.524 + 0.672\gamma/180)\sigma, \tag{16}$$

where $15^\circ \le \gamma \le 90^\circ$, $\sigma \le 0.25$. If the cavitator inclination angle $\delta_z \neq 0$, then the induced drag coefficient c_{xi} should be added in (15) (see below (24)).

The lift coefficient of the inclined cone cavitator c_y is calculated by the approximation formulae (22), (23) obtained according to our experimental results (see below in subsection 3.4).

Note that it follows from (23) that $c_{y0}^{\delta} = 0$ when $\beta_n = 86.85^\circ$. This value of the cone angle can be called a 'critical' one. Obviously, the cone cavitators with the cone angle close to the critical value cannot be used for the control of the cavitating vehicle motion.

There is the theoretical solution of the plane non-linear problem on cavitation flow over a wedge [27]. It gives qualitatively similar dependence $c_{y0}^{\alpha}(\gamma)$. In this case the critical value is $\beta_n = 101.17^\circ$.

2.2.3. Planing forces

The interaction between the model and the internal cavity wall is considered an unsteady planing of an elongated body along the curvilinear liquid boundary. Forces arising in this case are calculated based on both the principle of the plane sections and the Wagner's theory [1]. In this case, the solution of the problem on immersion of the circular arc through the curvilinear boundary is used [4, 19]:

$$F_{sy} = \rho\pi R_s^2 V \left[V_1 \frac{\bar{h}(2+\bar{h})}{(1+\bar{h})^2} + V_2 \frac{2\bar{h}}{1+K_c\bar{h}} \right], \tag{17}$$

where $\bar{h} = -h_k/(R_c - R_b)$, $k = 1, 2$, $h_1 < 0$, $h_2 < 0$ is the model transom immersion into the lower and upper cavity wall, respectively; V_1 is the transverse velocity of the model transom; V_2 is the velocity of the cavity wall; K_c is the correcting factor.

In the case of the arbitrary 3D motion, formula (17) may be applied to calculate the transversal components of the planing force F_{sy}, F_{sz} [11]. The skin friction force F_{sx} is calculated by the formula for turbulent boundary layer [38].

2.2.4. Fin forces

The considered model has a pair of symmetric horizontal fins creating the lift force F_{fy}, and a pair of symmetric vertical fins creating the lateral force F_{fz}. The fins have an arbitrary quadrangular shape in plan and a slender wedge shape in cross-sections.

In the case of the high-speed SC-models, the cavity-piercing fins are flown in the supercavitation regime. When varying the fin effective angle of attack α_f, stepwise changing of the lateral force may occur due to a change of the flow regime (like the base-cavitating wedge, or like the supercavitating plate), and the hysteresis effect [27, 28]. The total drag of fins F_{fx} consists of the cavitation drag and the skin friction drag.

Each of fins represents a wing having a relative aspect ratio $\lambda_f = h_f^2/S_f$, where h_f, S_f are the span and the wetted part area of the fin, respectively. As is known, in calculations a fin of arbitrary shape in plan may be replaced by an equivalent rectangular wing having the same area S_f, the same aspect ratio λ_f, and the chord $c_f = S_f/h_f$.

For the cavity-piercing fins, interference with the hull is absent. Therefore, they are considered isolated rectilinear hydrofoils with a small aspect ratio. The well-known methods of the linear theory of supercavitating underwater hydrofoils are used for calculating both the forces on the cavitating fins and the cavity shapes over fins [39–41]. The according relations are given, for example, in [10]. The lateral forces created by the horizontal and vertical fins are calculated by formulae:

$$F_{fy} = qS_{fh}c_{fy}(\alpha_{fh}), \qquad F_{fz} = qS_{fv}c_{fh}(\alpha_{fv}), \tag{18}$$

where c_{fy}, c_{fz} are the lift coefficients of horizontal and vertical fins, respectively; α_{fh} and α_{fv} are effective angles of attack of horizontal and vertical fins, respectively:

$$\alpha_{fh} = \delta_{fh} - \frac{V_y}{V} + \frac{\omega_z(x_{fh} - x_c)}{V}, \tag{19}$$

$$\alpha_{fv} = \delta_{fv} - \frac{V_z}{V} + \frac{\omega_y(x_{fv} - x_c)}{V}, \tag{20}$$

where δ_{fh} or δ_{fv} is the angle of defection of the fins relatively to the vehicle longitudinal plane, x_{fh} or x_{fv} are distances from the cavitator to the point of application of the lateral fin forces.

If the lateral forces on the fins of each pair are different, then an axial moment M_fx arises:

$$M_{fx} = F_{fz2}y_{fv2} - F_{fz1}y_{fv1} + F_{fy2}z_{fh2} - F_{fy1}z_{fh1}, \tag{21}$$

where z_{fh1}, z_{fh2}, y_{fv1}, y_{fv2} are distances from the points of application of forces F_{fy1}, F_{fy2}, F_{fz1}, F_{fz2}, respectively, to the model longitudinal axis. Here, indexes 1 and 2 are related to the lower and the upper vertical fins, and to the left and the right horizontal fins, respectively. This harmful moment may be compensated with a special small roll fin [9].

Finally, calculation of the hydrodynamic fin forces and moments is performed in the following sequence:

1) it is determined for each fin whether there is an intersection of the fin contour and the cavity walls;
2) if yes, the aspect ratio λ_f and the wetted area S_f of each fin are calculated;
3) the effective angle of attack α_f of each fin is calculated by formula (19) or (20);
4) type of flow over each fin is determined (like the base-cavitating wedge, or like the supercavitating plate);
5) for each fin, the force coefficients and coefficients of moment about the mass center are calculated;
6) coefficient of the total axial moment is calculated by formula (21);
7) for each fin, the fin cavity shape is calculated.

3. EXPERIMENTAL STUDY OF HYDRODYNAMIC FORCES ON THE CONE CAVITATORS

3.1. Laboratory instrumentation and measurement techniques

The experimental studies were carried using the high-speed towing tank at IHM NASU. The high-speed towing tank is 140 meters long, 4 meters wide and 1.8 meters deep. The experiments were organized in accordance with the ITTC resistance test methodology by towing model tests in the high-speed towing tank [42].

Water and air temperature was determined by a laboratory thermometer with uncertainty ±0.2°C and resolution 0.5°C. The density of water in the towing tank was determined by the water temperature and calculated according to the ITTC Procedure 7.5-02-01-03 [43]. The value of the gravity acceleration was taken at the latitude of the city of Kyiv. The experimental conditions are given in Tab. 1.

The air pressure in the cavity was measured through a drainage tube using a Freescale MPXV5004DP differential pressure sensor. The air pressure sensor is calibrated with a

reference pressure gauge. The relative uncertainty of the pressure sensor was less than 1.8%, which is close to ITTC recommendations 7.5-02-05-01 [42].

The lift was measured by a strain gauge system consisting of a strain gauge, strain gauge, and low pass filter. The strain gauge system was calibrated with reference weights. The relative uncertainty of the strain gauge system was $\leq 0.2\%$, which complies with ITTC recommendations 7.5-02-05-01 [42]. A differential pressure sensor and a strain gauge lift sensor were included in the automated data collection and processing system. The automated system for collecting and processing information was located on a towed cart and consisted of data acquisition devices (DAQ), an industrial computer, and a wireless adapter.

The angle of attack of the cavitator was measured by the photogrammetric method. The cavitator as part of the towed model was photographed with a digital non-metric camera for each angle of attack. The size of the photo was 5472 × 3080 pixels. Then, the frame was analyzed by the software package AutoCAD 2017 (Autodesk Inc.). To improve the accuracy and reduce systematic distortions of the image, the position of the cavitator on the optical axis of the lens of a digital non-metric camera and software methods were used. The uncertainty of the photogrammetric method was determined by measuring the exemplary angle (cavitator angle) and was no more than $\pm 0.3^\circ$ of the measured angle, which is close to the recommendations of ITTC 7.5-02-05-01 [42].

During the experiments, the average speed of the model was measured. The speed measurement system consisted of one photoelectric sensor and two reflectors. To measure the speed, the period between two pulses sent by the sensor was measured. Two reflectors were installed on the towed cart. The distance between the reflectors is known with an accuracy of

Tab. 1. Experimental conditions

Parameter	Designation	Dimension	Quantity	Uncertainty	
				absolute	relative
Water temperature	t_w	°C	16.5	±0.2	±0.012
Air temperature	t_{air}	°C	17.5	±0.2	±0.011
Gravity acceleration	g	m/s^2	9.8105	—	—
Water density	P	kg/m^3	999.20	±0.04	~ 0

Tab. 2. Uncertainty of measurements

Parameter	Designation	Dimension	Quantity	Uncertainty	
				absolute	relative
Pressure	Δp	Pa H/m^2	1128 1246	±20	±0.018 ±0.016
Model speed	V	m/s	9.122	±0.010	±0.001
Lift	F_y	N	10 . . . 20	±0.02	±0.002
Cavitator inclination angle	δ_z	degrees	7 14	±0.3	±0.04 ±0.02

0.9 mm. The period between two pulses was measured with a digital oscilloscope with a clock frequency of 20 MHz. The relative uncertainty in measuring the speed was less than 0.1%, which is in accordance with the recommendations of the ITTC procedure 7.5-02-05-01 [42].

The uncertainty of direct measurements of pressure in the cavity, lift, model velocity, and angle of attack of the cavitator are given in Tab. 2.

3.2. Description of the experimental setup and the cone cavitator models

In this work, the hydrodynamic characteristics of the cone cavitators with half-angles $\gamma = 20°$, $30°$, and $60°$ were tested. The disk cavitator was also used for comparison. Sketches of the cavitator models and their appearance are shown in Fig. 1.

Cavitators were mounted to the suspension shown in Fig. 2. The suspension was a hollow pylon. The top of the pylon was attached to the towing cart. The lower part of the pylon was connected to a horizontal tube with an outer diameter of 30 mm. Internal hollows of pylon and pipe had free communication.

A tensometric dynamometer with a threaded adapter was mounted into the nose of the horizontal tube. In experiments, a set of adapters was used. The adapters provided the attachment of the cavitator model with different angles of the cavitator inclination relative to the horizontal axis of the tube. In particular, threaded adapters were used that provided angles of inclination of $0°$, $\pm 7.5°$, and $\pm 14°$.

The aft part of the tube was plugged. In addition, a 4 mm diameter drainage tube was placed through the internal hollow of the pylon. The lower end of the drainage tube was led out into the cavity, the upper end of the drainage tube was connected to a pressure sensor.

The cavitation flow was formed by artificially blowing air into the zone behind the cavitator. The air supply to the cavity was forcibly carried out with the aid of a 6-step axial fan.

The immersion depth of the cavitator was regulated by the vertical movement of the pylon. During the experiments, the depth of the cavitator was set to $H = 150$ mm. In this case, as shown in [25], the effect of the free surface on the shape of the cavity behind the cavitator with a diameter of $D_n = 50$ mm is small.

All sensors and a dynamometer were included in the automated data acquisition and processing system of the high-speed towing tank [44].

3.3. Estimated parameters and calculated relations

During towing tests, the following parameters were determined:

- the cavitation number $\sigma = 2(p_w - p_c)/(\rho V^2)$;
- lift coefficient of the cavitator $c_y = F_{ny}/(qS_n)$, where F_{ny} is the cavitator lift force;
- drag coefficient of the cavitator $c_x = 2F_{nx}/(\rho V^2 S_n)$, where F_{nx} is the cavitator drag;
- the Froude number calculated by cavitator diameter $\mathrm{Fr} = V/\sqrt{gD_n}$;
- the volumetric air rate Q_v.

Experimental studies were conducted at approximately fixed the volumetric air rate $Q_v \approx (0.0064 \ldots 0.0072)$ m^3/s and the towing speeds $V \approx (8 \ldots 10)$ m/s. This air rate allowed,

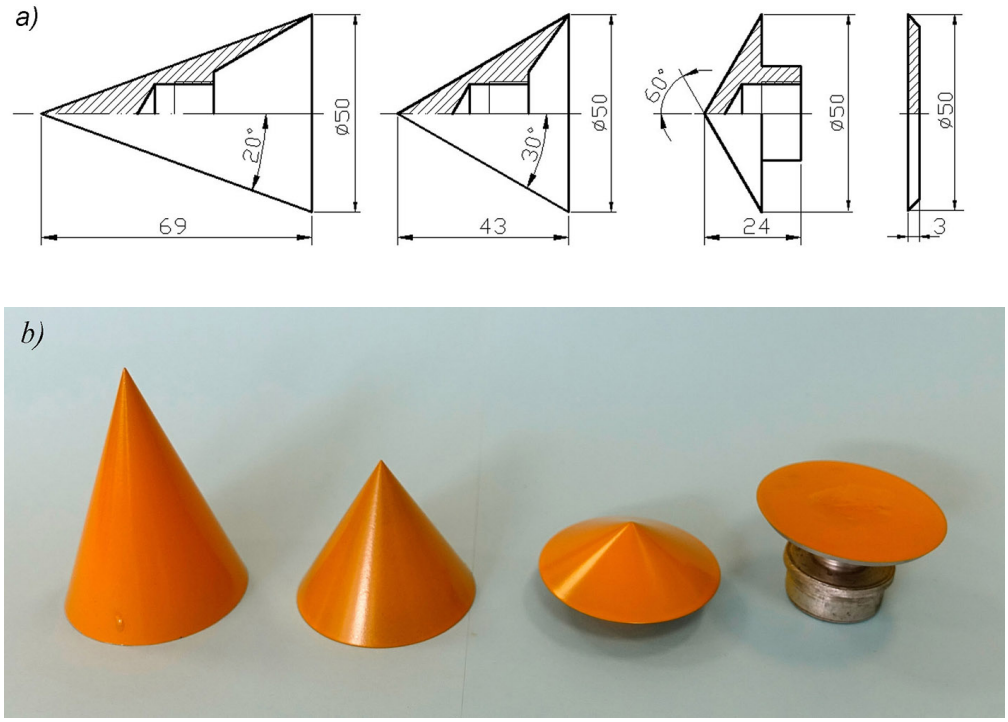

Fig. 1. Sketches (a) and appearance (b) of models of conical cavitators

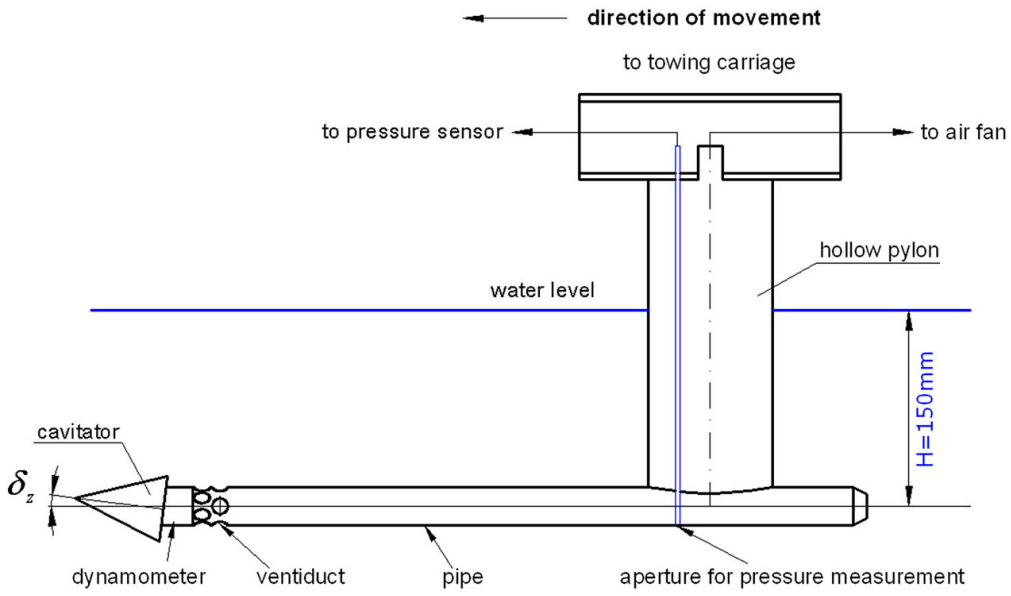

Fig. 2. Scheme of mounting the model of the cavitator to the towing system

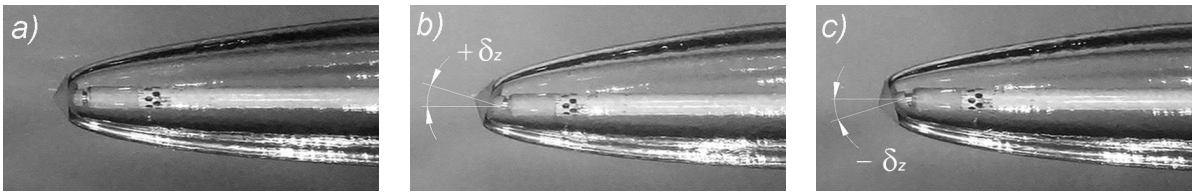

Fig. 3. Typical shape of the cavitation flow behind the cone cavitator with the half-angle $\gamma = 60°$: *a* — at zero inclination angle; *b* — at positive inclination angle; *c* — at negative inclination angle;

Tab. 3. Comparison of the value c_{y0}^{δ} of the disk cavitator

Source	[18]	[1]	IHM NASU
c_{y0}^{δ}, 1/rad	−0.7848	−0.7830	−0.7890

on the one hand, to achieve very low cavitation numbers $\sigma \approx (0.03 \dots 0.04)$, and on the other hand, to achieve a stable cavitation flow. In this case, the Froude numbers were Fr ≈ 11.5 to 14.3.

Typical appearances of the cavitation flow behind the cone cavitator depending on its orientation to the incoming flow are shown in Fig. 3.

3.4. Test results

In the work [45] it was concluded based on the results from [18] that the lift coefficient of the cone cavitator in the range of the inclination angle $-20° < \delta_z < 20°$ with sufficient practical accuracy can be represented as:

$$c_y = c_{y0}^{\delta}(1 + \sigma)\delta_z, \tag{22}$$

where c_{y0}^{δ} is the derivative of the cone cavitator lift coefficient with respect to the inclination angle δ_z when $\sigma = 0$. Therefore, the subject of our study was the parameter c_{y0}^{δ}. All results of measurements of the cavitator lift coefficient were processed in accordance with formula (22).

First of all, the results related to the disk cavitator were analyzed. In particular, this value was compared with the well-known results by Kichenyuk and Logvinovich. The results of comparison are given in Tab. 3. The values c_{y0}^{δ} are given in the table provided that the cavitator inclination angle is defined in radians. Comparison of the value c_{y0}^{δ} for the disk cavitator with the known results showed that the total measurement error in the experiment does not exceed 1%. Thus, the results of IHM NASU can be used to generate a universal dependence of the derivative of the lift coefficient with respect to the angle of inclination for different cone cavitator angles.

Similarly, the results of measurements of the lift coefficient of the cone cavitators were processed in accordance with formula (22). The processing results are given in Tab. 4.

Fig. 4 shows the dependence of the derivative of the lift coefficient on the cone cavitator half-angle $c_{y0}^{\delta} = f(\gamma)$. In constructing this dependency, the results by Kiceniuk1954) were used as well. In addition, when plotting the dependence in Fig. 4 also takes into account that the cone degenerates into a cylinder if $\gamma \to 0°$. For a cylinder at zero cavitation number

Tab. 4. The value c_{y0}^{δ} of the cone cavitators

γ	20°	30°	60°
c_{y0}^{δ}, 1/rad	0.8354	0.4950	−0.4060

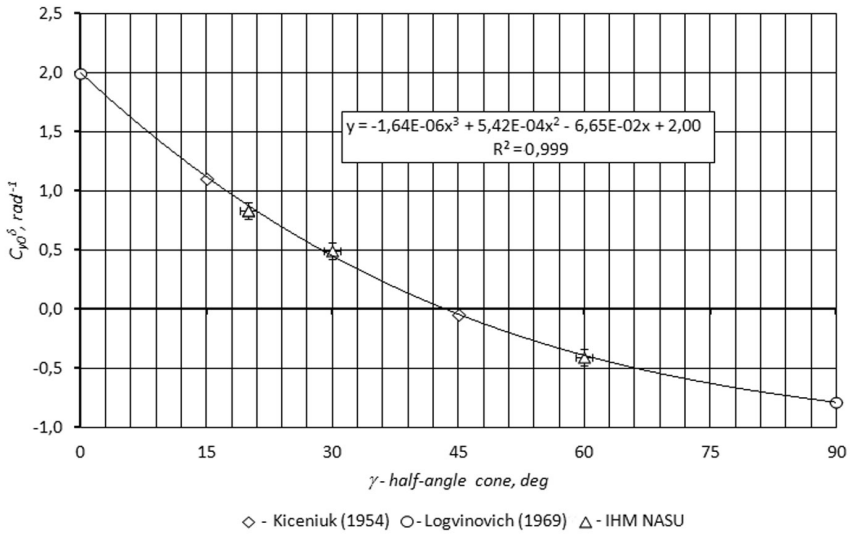

Fig. 4. Dependence of the derivative of the lift coefficient on the cone half-angle $c_{y0}^{\delta} = f(\gamma)$

$c_{y0}^{\delta} = 2$ [1]. If $\gamma \to 90°$ then the cone degenerates into a disk. For a disk with zero cavitation number $c_{y0}^{\delta} = 0.783$ if the inclination angle is given in radians [1].

The dependence $c_{y0}^{\delta} = f(\gamma)$ shown in Fig. 4 can be approximated by a third degree polynomial:

$$c_{y0}^{\alpha} = 2 - 1.64 \cdot 10^{-6}\gamma^3 + 5.42 \cdot 10^{-}4\gamma^2 – 6.65 \cdot 10^{-2}\gamma. \tag{23}$$

There is a large number of works in which simple approximation formulae were obtained for calculating the drag coefficient of cone cavitators (see, for example, [3, 46]. Unfortunately, most of the known results refer to the case of motion with a zero inclination angle of the cavitator.

If we consider the cavitator as a control surface (for example, a wing with an extremely small aspect ratio), then an induced drag should also arise on it when a lift arises. In the article [45] it was concluded based on the analysis of the results by Kiceniuk [18] that this induced drag is proportional to both the lift coefficient c_y and $\sin\delta_z$.. Thus, the drag coefficient of the cone cavitator c_x can be represented as:

$$c_x = c_x^{(}0) + c_x i, \qquad c_x i = c_y \sin\delta_z, \tag{24}$$

where $c_x^{(0)}$ is the cavitation drag coefficient when $\delta_z = 0$; c_{xi} is the induced drag coefficient. In this work, the coefficient $c_x^{(0)}$ is calculated using the approximation formula (16), which gives satisfactory results in the range of the cone cavitator half-angle $15° \le \gamma \le 90°$ for cavitation numbers $\sigma \le 0.25$. The viscous component of the drag for the considered cone angles is negligible.

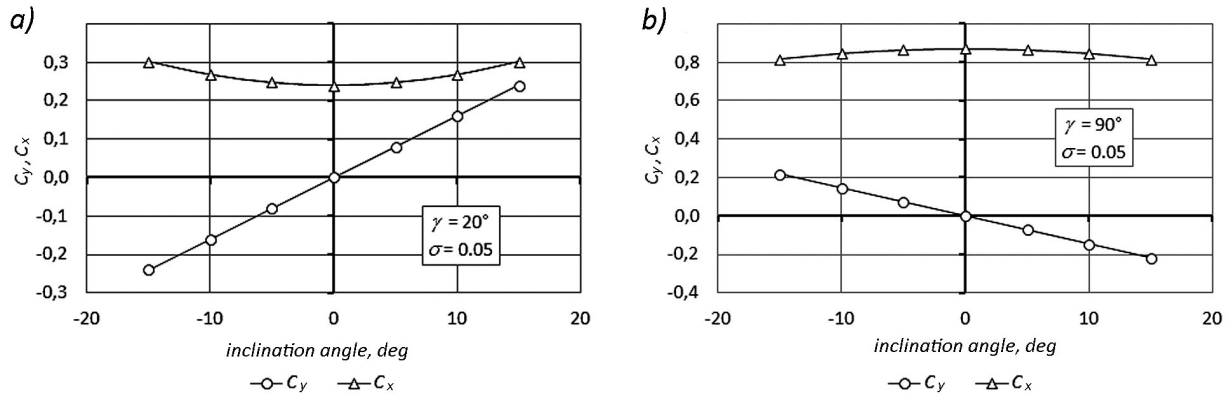

Fig. 5. Typical dependences of the hydrodynamic force coefficients:
a — for the cone cavitator; *b* — for the disk cavitator

Thus, formulae (22)—(24) make it possible to calculate the coefficients of the hydrodynamic forces on the cone cavitators at the arbitrary non-zero inclination angles. As an example, Fig. 5 shows a typical view of the dependences of both the lift coefficient and the drag coefficient of the cone cavitator with the half-angles $\gamma = 20°$ and $\gamma = 90°$ (disk cavitator) with the cavitation number $\sigma = 0.05$.

4. EXPERIMENTAL STUDY OF THE CAVITY SHAPE BEHIND THE CONE CAVITATORS

Formulae for a composite cavity by G. V. Logvinovich (1), (2) are the most reliable for analysis of the shape of steady axisymmetric cavities. These formulae agree with experimental data for the disk cavitators. To calculate the shape of the cavity behind the cone cavitators, the method of an equivalent disk cavitator is used (see above, paragraph 2.1.2). In this case, to calculate the shape of the cavity forward section, we used an approximation formula (7) instead of (1).

The verification of this approach is carried out by comparing the calculated parameters of the cavitation flow with similar parameters obtained in the towing tests of the SC-vehicle model.

4.1. Description of the experimental setup and the SC-vehicle model

The general view and dimensions of the schematized SC-vehicle model are shown in Fig. 6. The dimensions of the SC-model were chosen taking into account the capabilities of the towing system of the towing tank to obtain reliable results. The shape of the model body was a combination of conical and cylindrical surfaces. The cylindrical surface had a diameter of 80 mm and a length of 200 mm. The model was hollow. Inside the model, several lead weights were moving along its length, which served to balance the model concerning a given mass center.

In the nose part of the model, a special threaded adapter was provided for mounting the cavitator. To verify the shape of the cavity, the cone cavitator with a base diameter of 50 mm and a half-angle of 20° was used. The threaded adapter also provided the required angle of the cavitator inclination.

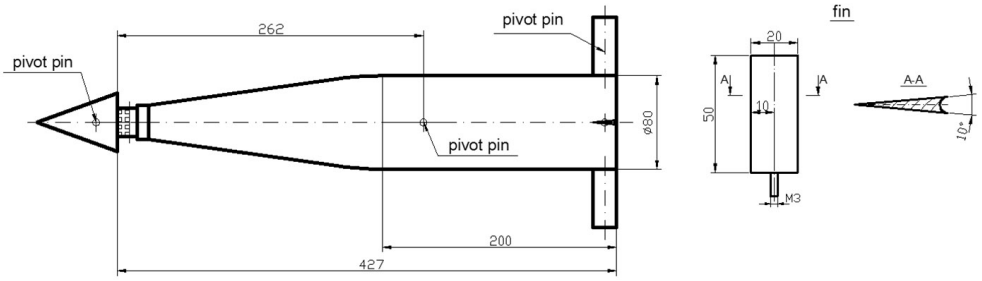

Fig. 6. General view and dimensions of the schematized SC-vehicle model

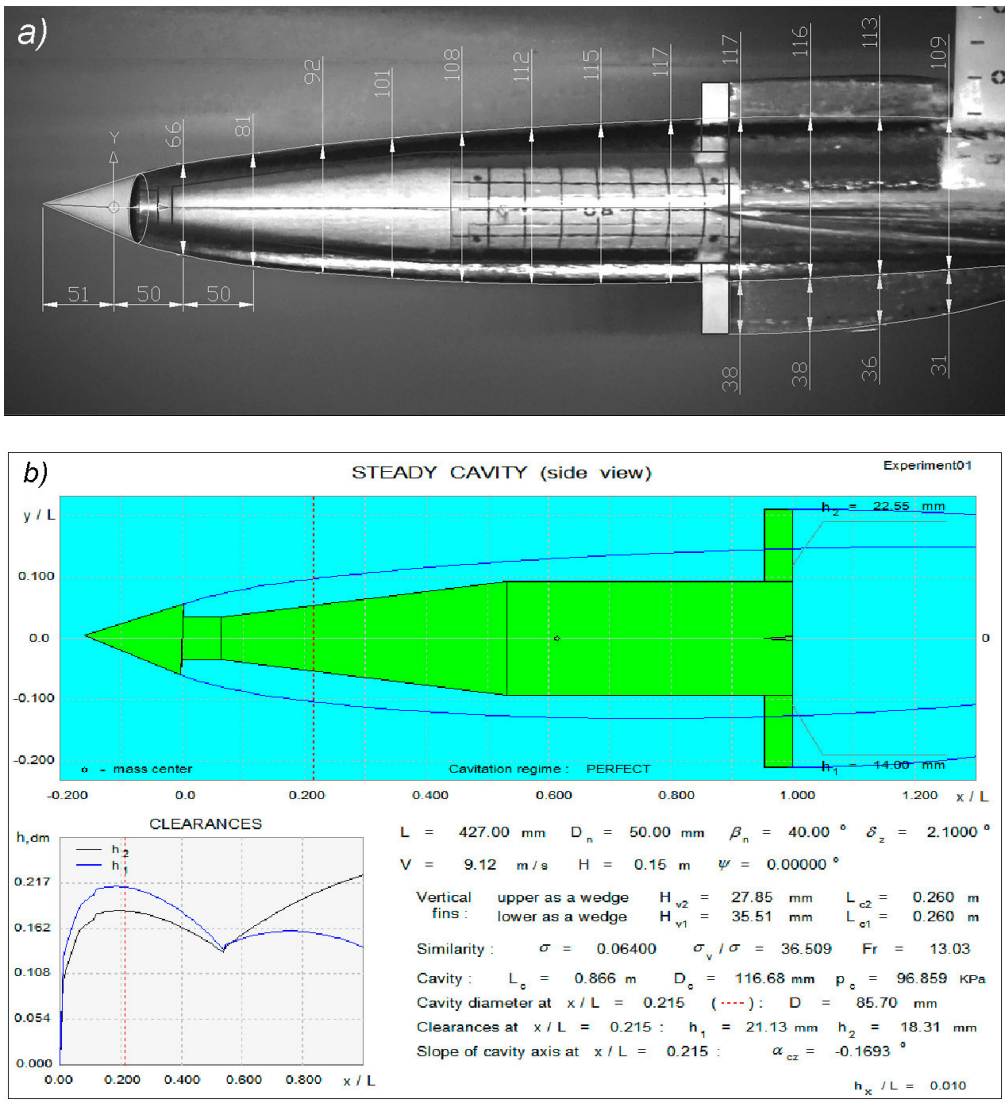

Fig. 7. A typical view of the cavitation flow around an SC-vehicle model with a conical cavitator:

a — experiment; *b* — simulation

Tab. 5. Comparison of the cavity dimensions obtained by calculations and experiments

Section No.	Distance, mm	Diameter, mm		Divergence of results, %
		calculation	experiment	
1.	50	66.9	66	+1.36
2.	100	83.3	81	+2.72
3.	150	94.0	92	+2.17
4.	200	102.1	101	+1.09
5.	250	108.2	108	+0.19
6.	300	112.5	112	+0.45
7.	350	115.2	115	+0.17
8.	400	116.5	117	−0.43
9.	450	116.5	117	−0.43
10.	500	115.0	116	−0.86
11.	550	112.2	113	−0.71

In the aft part of the model, the rotary vertical and horizontal fins were installed. The fins had wedge-shaped cross-sections (see Fig. 6).

To determine the geometric parameters of the cavitation flow during the experiments the underwater video filming in the coordinates associated with the towing carriage was used. To organize underwater video filming, a water-proof container was moving parallel to the model, in which a remotely controlled video camera and lighters were placed.

4.2. Test results

To verify the calculation formulae and relations used to determine the shape and size of the cavity, the SC-model towing tests were carried out at a towing speed of 9.12 m/s with a zero pitch angle ψ. In this case, the cavitator inclination angle was $\delta_z = 2.1°$. The results of these tests are shown in Fig. 7a. Similar calculations of the cavitation flow around the schematized SC-vehicle model were also carried out, the results are shown in Fig. 7b.

Tab. 5 shows the results of comparing the dimensions of the cavity obtained by calculation and in the experiment. Comparison of the shape and size of cavities obtained by calculation and in experiment shows that their deviation does not exceed ±3%.

5. EXPERIMENTAL STUDY OF THE SUPERCAVITATING MODEL DYNAMICS

During experimental tests of the model dynamics, the SC-model could perform free oscillations in pitch in the longitudinal-vertical plane. The model was mounted to the pylon of the towing system, the design scheme of which is shown in Fig. 8. The pylon was connected to the SC-model using a flexible elastic corrugated hose, which allowed the model to rotate free in the longitudinal-vertical plane about the suspension point. The suspension point of the model coincided with its mass center.

By choosing both the cavitator inclination angle and the horizontal fin deflection angle, the following stationary and non-stationary modes of motion of the SC-model were modeled:

The mode of the model motion with planing along the upper cavity wall.

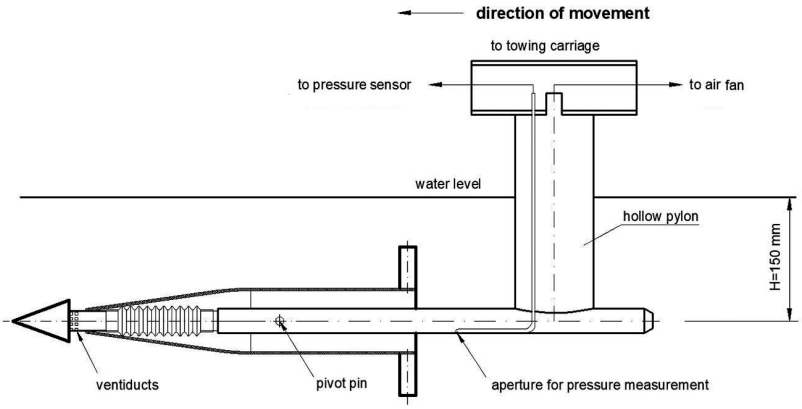

Fig. 8. Scheme of mounting the SC-vehicle model to the towing system

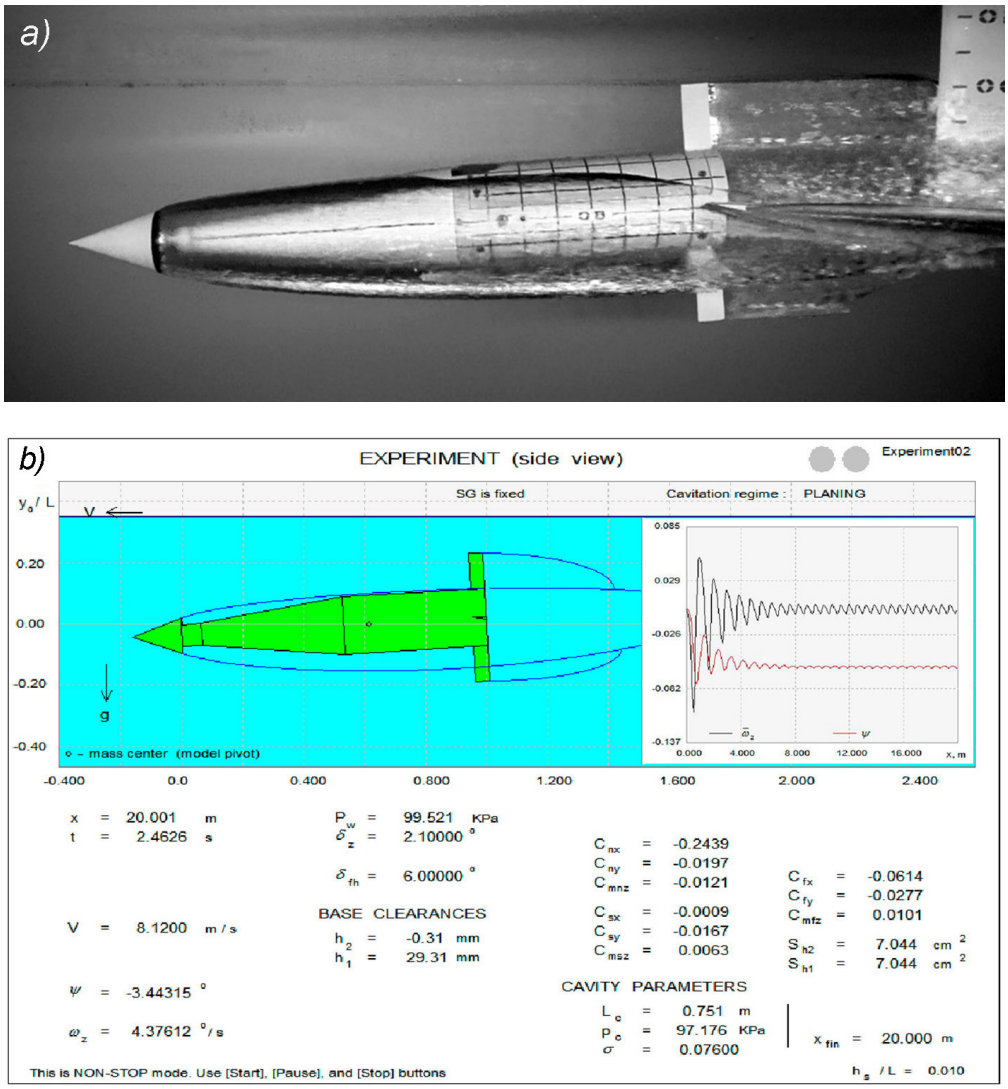

Fig. 9. Motion of the SC-model with planing along the upper cavity wall:

a — experiment; b — simulation

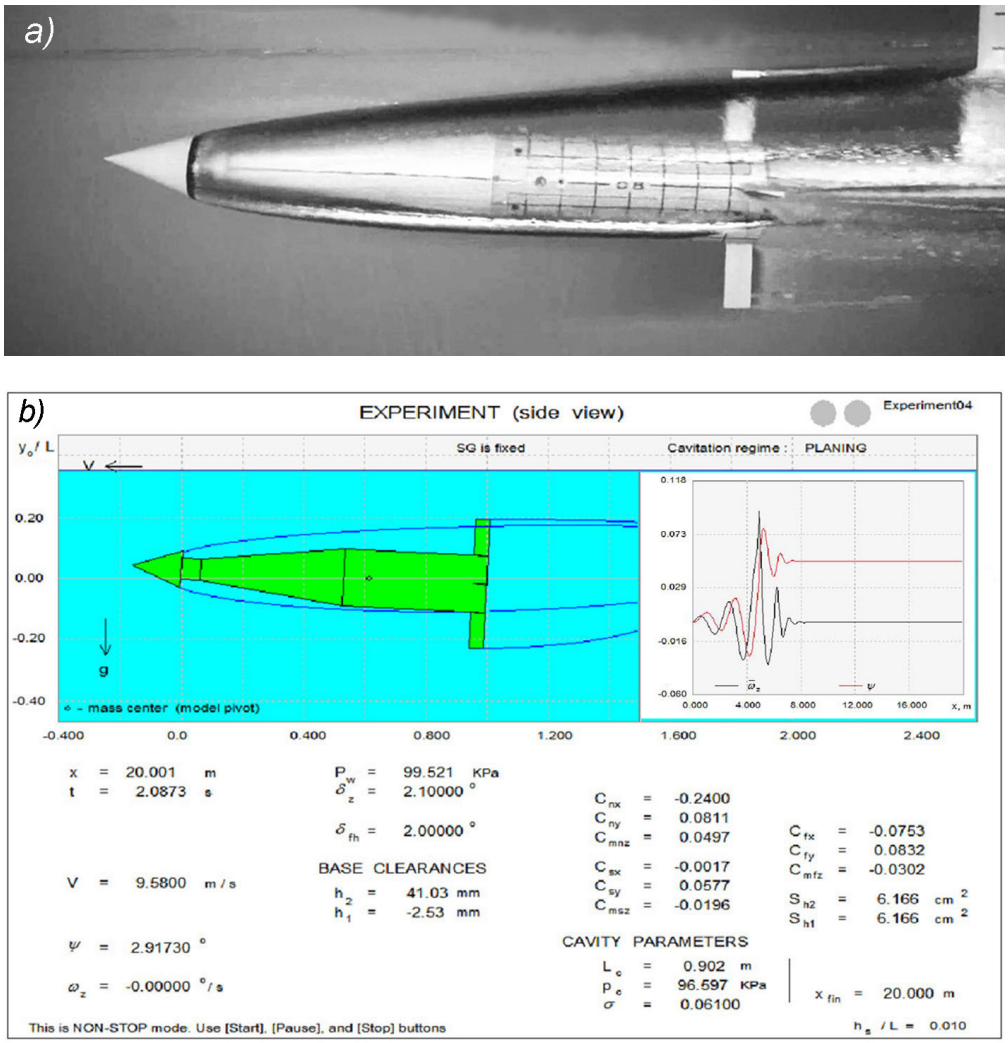

Fig. 10. Motion of the SC-model with planing along the bottom cavity wall:

a — experiment; b — simulation

This mode of motion was performed at the cavitator inclination angle $\delta_z = 2.1°$ and the fin deflection angle$\delta_{fh} = 6.0°$. In this mode, the model performs several damped oscillations and enters the mode of steady motion with the pitch angle of about $\psi = -3.4°$. A typical form of the model motion in this mode at the computer simulation and in the experiment is shown in Fig. 9.

The mode of the model motion with planing along the bottom cavity wall.

This mode of motion was performed at the cavitator inclination angle $\delta_z = 2.1°$ and the fin deflection angle $\delta_{fh} = 2.0°$. In this mode, the model performs several damped oscillations and stabilizes in a stationary mode of planing along the bottom cavity wall with the pitch angle of about $\psi = 2.9°$. A typical form of the model motion in this mode at the computer simulation and in the experiment is shown in Fig. 10.

The mode of the model motion with ricocheting from the upper and lower cavity walls.

This mode of motion was performed at the cavitator inclination angle $\delta_z = 2.1°$ and the

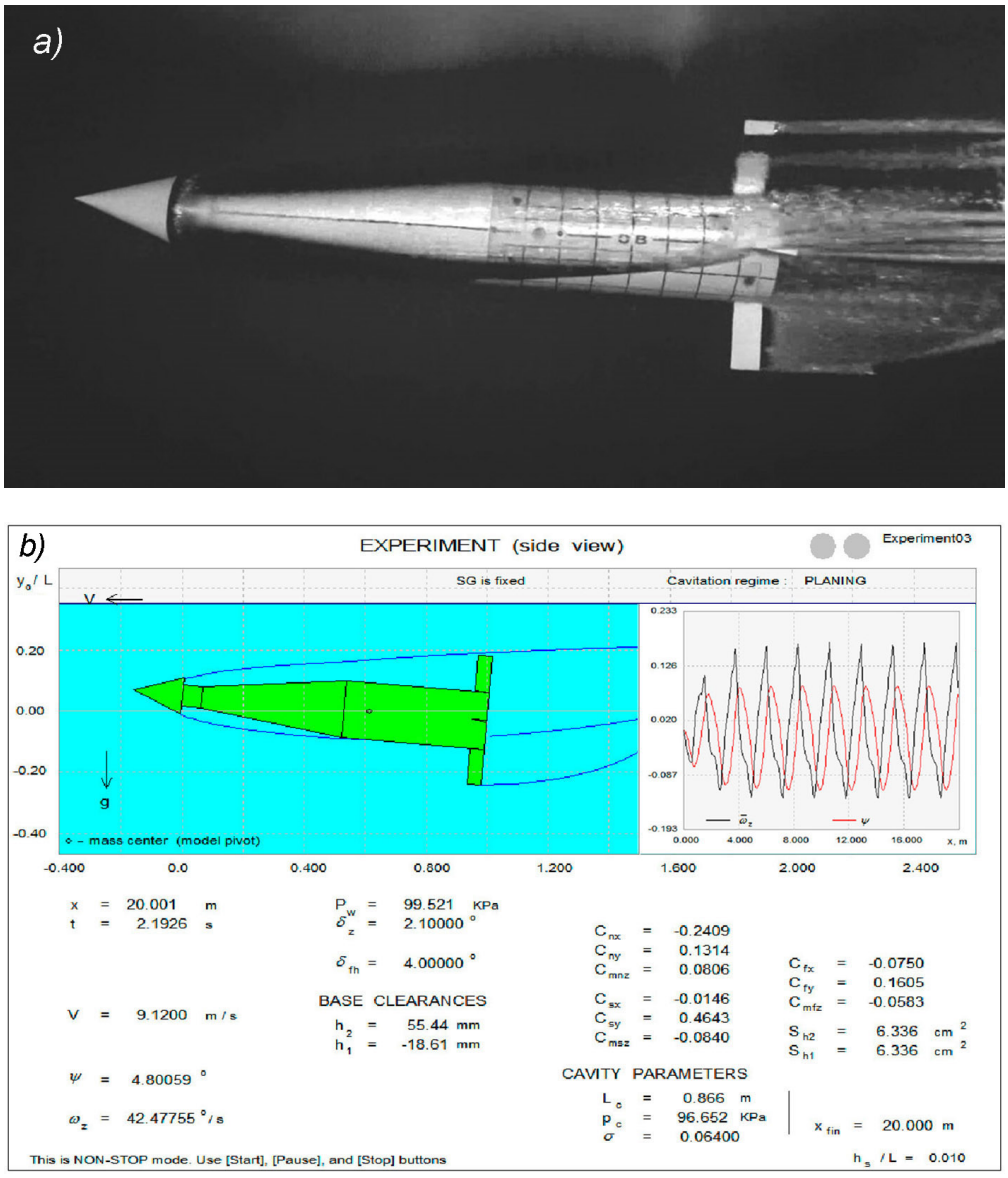

Fig. 11. Motion of the SC- model with ricocheting from the upper and bottom cavity walls:

a — experiment; b — simulation

fin deflection angle $\delta_{fh} = 4.0°$. In this mode, the model performs steady angular oscillations, ricocheting by turns from the upper and lower cavity walls, between the values $\psi = -5.41°$ and 4.93° with the frequency $f = 4.6$ Hz. A typical form of the model motion in this mode at the computer simulation and in the experiment is shown in Fig. 11.

As can be seen for all three modes, the calculated and the experimentally observed kinematic parameters of the model closely correspond to each other.

6. CONCLUSIONS

A series of experimental studies were carried out to verify the approximation mathematical model, which is used at the Institute of Hydromechanics of the NAS of Ukraine for

computer simulation of the SC-vehicle dynamics. The main attention is paid to the dynamics of supercaviting models with cone cavitators.

To calculate the shape of the cavities behind the cone cavitators, the equivalent disk method was used. To calculate the shape of the forward part of the cavity, we propose the new approximation formula (7).

Based on the results of experimental studies, the new approximation formula (23) for the lift on the inclined cone cavitators is proposed. This formula is convenient for use in algorithms of computer simulation of the SC-vehicle guided motion.

Comparison of the shapes of steady and unsteady cavities behind the inclined cone cavitators, obtained by calculation and in the experiment, showed their good agreement.

The verification of the mathematical model 'as a whole' was carried out by comparing the calculated kinematic parameters with similar parameters obtained during towing tests of the movable SC-model having one degree of freedom in pitch.

The close agreement of the kinematic characteristics of the movable SC-model, obtained by calculation and in the experiment, indirectly testifies to the sufficient accuracy of the formula (17) used for calculating the planing force, and also formulae used for calculating the cavity-piercing fin forces.

In general, it can be concluded that the developed mathematical model allows the dynamic behavior of the underwater SC-vehicles to be predicted adequately and with sufficient accuracy for practice.

REFERENCES

[1] G. V. Logvinovich, *Hydrodynamics of flows with free boundaries*. Kyiv: Naukova Dumka, 1969.

[2] Y. N. Savchenko and G. Y. Savchenko, "Estimation of efficiency of using the supercavitation on the axisymmetric hulls," *Applied Hydromechanics*, vol. 6(78), no. 4, pp. 78–83, 2004.

[3] L. G. Guzevsky, "Numerical and analytical analysis of cavitation flows," *Applied Hydromechanics*, vol. 15(87), no. 1, pp. 33–44, 2013.

[4] E. V. Paryshev, "On unsteady planing of a body over liquid curvilinear surface," in *The Second International Summer Scientific School 'High Speed Hydrodynamics'*, Cheboksary, 2004, pp. 175–178.

[5] V. N. Semenenko, "Some problems of supercavitating vehicle designing," in *Proceedings of the International Conference on superfast marine vehicles moving above, under and in water surface (SuperFAST'2008)*, Saint Petersburg, 2008.

[6] Y. N. Savchenko and V. N. Semenenko, "Motion of supercavitating vehicle during underwater speeding-up," *Applied Hydromechanics*, vol. 17(89), no. 4, pp. 36–42, 2015.

[7] V. N. Semenenko and O. I. Naumova, "Dynamics of a partially cavitating underwater vehicle," *Hydrodynamics and Acoustics*, vol. 1(91), no. 1, pp. 70–84, 2018. DOI: https://doi.org/10.15407/jha2018.01.070

[8] V. N. Semenenko and Y. I. Naumova, *Study of the supercavitating body dynamics*. Springer Berlin Heidelberg, 2011, pp. 147–176. DOI: https://doi.org/10.1007/978-3-642-23656-3_9

[9] V. N. Semenenko and O. I. Naumova, "Some ways of hydrodynamic fin application for underwater supercavitating vehicles," *Hydrodynamics and Acoustics*, vol. 1(91), no. 3, pp. 355–371, 2018. DOI: https://doi.org/10.15407/jha2018.03.355

[10] V. N. Semenenko, "Prediction of supercavitating vehicle maneuvering," in *Proceediings of the 11th International Summer Scientific School 'High Speed Hydrodynamics and Shipbuilding (HSH-2013)'*, Cheboksary, 2013, pp. 181–190.

[11] Y. N. Savchenko, V. N. Semenenko, and G. Y. Savchenko, "Peculiarities of supercavitating vehicles' maneuvering," *International Journal of Fluid Mechanics Research*, vol. 46, no. 4, pp. 309–323, 2019. DOI: https://doi.org/10.1615/interjfluidmechres.v46.i4.30

[12] V. N. Semenenko, "Computer modeling of pulsations of ventilated supercavities," *International Journal of Fluid Mechanics Research*, vol. 23, no. 3-4, pp. 302–312, 1996. DOI: https://doi.org/10.1615/interjfluidmechres.v23.i3-4.140

[13] J. Dzielski and A. Kurdila, "A benchmark control problem for supercavitating vehicles and an initial investigation of solutions," *Journal of Vibration and Control*, vol. 9, no. 7, pp. 791–804, 2003. DOI: https://doi.org/10.1177/1077546303009007004

[14] V. Nguyen and B. Balachandran, "Supercavitating vehicles with noncylindrical, nonsymmetric cavities: dynamics and instabilities," *Journal of Computational and Nonlinear Dynamics*, vol. 6, no. 4, 2011. DOI: https://doi.org/10.1115/1.4003408

[15] S. Kim and N. Kim, "Integrated dynamics modeling for supercavitating vehicle systems," *International Journal of Naval Architecture and Ocean Engineering*, vol. 7, no. 2, pp. 346–363, 2015. DOI: https://doi.org/10.1515/ijnaoe-2015-0024

[16] D. R. Stinebring and J. W. Holl, "Water tunnel simulation study of the later stages of water entry of conical head bodies," ARL Penn State, Tech. Rep. TM-79-206, 1979.

[17] V. Farhangmehr and M. H. Dashti, "Experimental investigation on the supercavitating flows over a cylindrical body with conical cavitators," *International Journal of Science, Engineering and Technology Research*, vol. 5, no. 7, pp. 2353–2365, 2016.

[18] T. Kiceniuk, "An experimental study of the hydrodynamic forces acting on family of cavity-producing conical bodies of revolution inclined to the flow," Hydrodynamics Laboratory, California Institute of Technology, Pasadena, CA, Report E-12-17, 1954.

[19] G. V. Logvinovich, "Some problems on planing," *Trudy TsAGI*, no. 2052, pp. 3–12, 1980.

[20] A. D. Vasin and E. V. Paryshev, "Immersion of a cylinder in liquid through a cylindrical free surface," *Fluid Dynamics*, vol. 36, no. 2, pp. 169–177, 2001. DOI: https://doi.org/10.1023/a:1019299930896

[21] M. Mirzaei, M. Eghtesad, and M. M. Alishahi, "Planing force identification in high-speed underwater vehicles," *Journal of Vibration and Control*, vol. 22, no. 20, pp. 4176–4191, 2016. DOI: https://doi.org/10.1177/1077546315571660

[22] Y. F. Zhuravlev, O. P. Shorygin, and N. A. Shulman, "On the lift of the planning cylinder," *Uchenye Zapiski TsAGI*, vol. 10, no. 6, pp. 113–117, 1979.

[23] Y. N. Savchenko and G. Y. Savchenko, "Cylinder gliding on the supercavern surface," *Applied Hydromechanics*, vol. 9(81), no. 1, pp. 81–85, 2007.

[24] J. Dzielski, P. Sammut, and R. Datla, "Planing-hull forces and moments on a cylindrical body in a cavity," in *Proceedings of the 8th International Symposium on Cavitation*, ser. CAV. Singapore: Research Publishing Services, 2012, p. 928–932. DOI: https://doi.org/10.3850/978-981-07-2826-7_285

[25] V. V. Serebryakov, V. V. Moroz, V. V. Kochin, and J. E. Dzielski, "Experimental study on planing motion of a cylinder at angle of attack in the cavity formed behind an axisymmetric cavitator," *Journal of Ship Research*, vol. 64, no. 2, pp. 139–153, 2019. DOI: https://doi.org/10.5957/josr.09180077

[26] Y. N. Savchenko, V. N. Semenenko, and G. Y. Savchenko, "Features of manoeuvring at the supercavitation flowing around," *Applied Hydromechanics*, vol. 18(90), no. 1, pp. 79–82, 2016.

[27] V. N. Semenenko and Y. N. Savchenko, "Special features of supercavitating flow around polygonal contours," *International Journal of Fluid Mechanics Research*, vol. 28, no. 5, pp. 660–672, 2001. DOI: https://doi.org/10.1615/InterJFluidMechRes.v28.i5.60

[28] M. Wosnik and R. E. A. Arndt, "Control experiments with a semi-axisymmetric supercavity and a supercavity-piercing fin," in *Proceedings of the Seventh International Symposium on Cavitation (CAV2009)*, Ann Arbor, MI, 2009.

[29] Y. N. Savchenko, Y. D. Vlasenko, and G. Y. Savchenko, "Action of a rudder on a planing hull," *Applied Hydromechanics*, vol. 17(89), no. 3, pp. 67–70, 2015.

[30] D. E. Sanabria, G. Balas, and R. Arndt, "Modeling, control, and experimental validation of a high-speed supercavitating vehicle," *IEEE Journal of Oceanic Engineering*, vol. 40, no. 2, pp. 362–373, 2015. DOI: https://doi.org/10.1109/joe.2014.2312591

[31] A. McNitt, J. Dzielski, and D. Stinebring, "Experimental validation of planing models for a supercavitating vehicle," in *UDT Pacific 2006 Conference Proceedings*, San Diego, CA, 2006, the Applied Research Laboratory of Pennsylvania State University.

[32] V. N. Semenenko, "Artificial cavitation. physics and calculations," VKI, Brussels, RTO-AVT/VKI Special Course on Supercavitating Flows, 2001.

[33] V. N. Buyvol, *Slender cavities in flows with perturbations*. Kyiv: Naukova Dumka, 1980.

[34] L. A. Epshtein, *Methods of the theory of dimensionalities and similarity in problems of ship hydromechanics*. Leningrad: Sudostroenie, 1970.

[35] G. V. Logvinovich and V. V. Serebryakov, "On methods for calculating the shape of slender axisymmetric cavities," *Gidromehanika*, vol. 32, no. 47–54, 1975.

[36] G. V. Logvinovich, "Problems of the theory of slender axisymmetric cavities," *Trudy TsAGI*, no. 1797, pp. 3–17, 1976.

[37] E. V. Paryshev, "Theoretical investigation of stability and pulsation of axisymmetric cavities," *Trudy TsAGI*, no. 1907, pp. 17–40, 1978.

[38] H. Schlichting, *Boundary layer theory*. Oxford: Pergamon Press, 1956.

[39] M. P. Tulin, "Steady two-dimensional cavity flows about slender bodies," David Taylor Model Basin, Tech. Rep. 834, 1953.

[40] I. I. Yefremov, *Linearized theory of cavitation flow*. Kyiv: Institute of Hydromechanics of AS UkrSSR, 1974.

[41] I. T. Yegorov, Y. M. Sadovnikov, I. I. Isaev, and M. A. Basin, *Artificial cavitation*. Leningrad: Sudostroenie, 1971.

[42] "Resistance test. high speed marine vehicles. testing and extrapolation methods," ITTC, Recommended Procedures and Guidelines 7.5-02 -05-01, 2008.

[43] "Fresh water seawater properties," ITTC, Recommended Procedures and Guidelines 7.5-02-01-03, 2011.

[44] V. A. Kochin and V. V. Moroz, "Automated data acquisition and processing system for a high-speed towing tank," *Modern Automation Technologies*, no. 3, pp. 48–50, 2009.

[45] A. May, "Water entry and the cavity-running behavior of missiles," Naval Surface Weapons Center, White Oak Laboratory, Silver Spring, MD, Tech. Rep. 75-2, 1975.

[46] V. V. Serebryakov, "A drag of axisymmetric cavitators at low cavitation numbers," *Applied Hydromechanics*, vol. 16(88), no. 4, pp. 54–65, 2014.

ЛІТЕРАТУРА

[1] Логвинович Г. В. Гидродинамика течений со свободными границами. — Киев : Наукова думка, 1969. — 208 с.

[2] Савченко Ю. Н., Савченко Г. Ю. Оценка эффективности использования суперкавитации на осесимметричных корпусах // Прикладна гідромеханіка. — 2004. — Т. 6(78), № 4. — С. 78–83.

[3] Гузевский Л. Г. Численный и аналитический анализ кавитационных течений // Прикладна гідромеханіка. — 2013. — Т. 15(87), № 1. — С. 33–44.

[4] Paryshev E. V. On unsteady planing of a body over liquid curvilinear surface // The Second International Summer Scientific School 'High Speed Hydrodynamics'. — Cheboksary. — 2004. — P. 175–178.

[5] Semenenko V. N. Some problems of supercavitating vehicle designing // Proceedings of the International Conference on superfast marine vehicles moving above, under and in water surface (SuperFAST'2008). — Saint Petersburg. — 2008.

[6] Савченко Ю. Н., Семененко В. Н. Движение суперкавитирующего аппарата на подводном участке разгона // Прикладна гідромеханіка. — 2015. — Т. 17(89), № 4. — С. 36–42.

[7] Semenenko V. N., Naumova O. I. Dynamics of a partially cavitating underwater vehicle // Гідродинаміка і акустика. — 2018. — Т. 1(91), № 1. — С. 70–84.

[8] Semenenko V. N., Naumova Y. I. Study of the supercavitating body dynamics // Supercavitation: Advances and Perspectives. — Springer Berlin Heidelberg, 2011. — P. 147–176.

[9] Semenenko V. N., Naumova O. I. Some ways of hydrodynamic fin application for underwater supercavitating vehicles // Гідродинаміка і акустика. — 2018. — Т. 1(91), № 3. — С. 355–371.

[10] Semenenko V. N. Prediction of supercavitating vehicle maneuvering // Proceediings of the 11th International Summer Scientific School 'High Speed Hydrodynamics and Shipbuilding (HSH-2013)'. — Cheboksary. — 2013. — P. 181–190.

[11] Savchenko Y. N., Semenenko V. N., Savchenko G. Y. Peculiarities of supercavitating vehicles' maneuvering // International Journal of Fluid Mechanics Research. — 2019. — Vol. 46, no. 4. — P. 309–323.

[12] Semenenko V. N. Computer modeling of pulsations of ventilated supercavities // International Journal of Fluid Mechanics Research. — 1996. — Vol. 23, no. 3-4. — P. 302–312.

[13] Dzielski J., Kurdila A. A benchmark control problem for supercavitating vehicles and an initial investigation of solutions // Journal of Vibration and Control. — 2003. — Vol. 9, no. 7. — P. 791–804.

[14] Nguyen V., Balachandran B. Supercavitating vehicles with noncylindrical, nonsymmetric cavities: dynamics and instabilities // Journal of Computational and Nonlinear Dynamics. — 2011. — Vol. 6, no. 4.

[15] Kim S., Kim N. Integrated dynamics modeling for supercavitating vehicle systems // International Journal of Naval Architecture and Ocean Engineering. — 2015. — Vol. 7, no. 2. — P. 346–363.

[16] Water tunnel simulation study of the later stages of water entry of conical head bodies : Rep. : TM-79-206 / ARL Penn State ; executor: Stinebring D. R., Holl J. W. : 1979.

[17] Farhangmehr V., Dashti M. H. Experimental investigation on the supercavitating flows over a cylindrical body with conical cavitators // International Journal of Science, Engineering and Technology Research. — 2016. — Vol. 5, no. 7. — P. 2353–2365.

[18] An experimental study of the hydrodynamic forces acting on family of cavity-producing conical bodies of revolution inclined to the flow : Report : E-12-17 / Hydrodynamics Laboratory, California Institute of Technology ; executor: Kiceniuk T. — Pasadena, CA : 1954.

[19] Логвинович Г. В. Некоторые вопросы глиссирования // Труды ЦАГИ. — 1980. — № 2052. — С. 3–12.

[20] Vasin A. D., Paryshev E. V. Immersion of a cylinder in liquid through a cylindrical free surface // Fluid Dynamics. — 2001. — Vol. 36, no. 2. — P. 169–177.

[21] Mirzaei M., Eghtesad M., Alishahi M. M. Planing force identification in high-speed underwater vehicles // Journal of Vibration and Control. — 2016. — Vol. 22, no. 20. — P. 4176–4191.

[22] Журавлев Ю. Ф., Шорыгин О. П., Шульман Н. А. О подъемной силе глиссирующего цилиндра. // Ученые записки ЦАГИ. — 1979. — Т. 10, № 6. — С. 113–117.

[23] Савченко Ю. Н., Савченко Г. Ю. Глиссирование цилиндра по поверхности суперкаверны // Прикладна гідромеханіка. — 2007. — Т. 9(81), № 1. — С. 81–85.

[24] Dzielski J., Sammut P., Datla R. Planing-hull forces and moments on a cylindrical body in a cavity // Proceedings of the 8th International Symposium on Cavitation. — Singapore : Research Publishing Services. — 2012. — CAV. — P. 928–932.

[25] Experimental study on planing motion of a cylinder at angle of attack in the cavity formed behind an axisymmetric cavitator / Serebryakov V. V., Moroz V. V., Kochin V. V., and Dzielski J. E. // Journal of Ship Research. — 2019. — Vol. 64, no. 2. — P. 139–153.

[26] Савченко Ю. Н., Семененко В. Н., Савченко Г. Ю. Особенности маневрирования при суперкавитационном обтекании // Прикладна гідромеханіка. — 2016. — Т. 18(90), № 1. — С. 79–82.

[27] Semenenko V. N., Savchenko Y. N. Special features of supercavitating flow around polygonal contours // International Journal of Fluid Mechanics Research. — 2001. — Vol. 28, no. 5. — P. 660–672.

[28] Wosnik M., Arndt R. E. A. Control experiments with a semi-axisymmetric supercavity and a supercavity-piercing fin // Proceedings of the Seventh International Symposium on Cavitation (CAV2009). — Ann Arbor, MI. — 2009.

[29] Савченко Ю. Н., Власенко Ю. Д., Савченко Г. Ю. Работа руля на глиссирующем корпусе // Прикладна гідромеханіка. — 2015. — Т. 17(89), № 3. — С. 67–70.

[30] Sanabria D. E., Balas G., Arndt R. Modeling, control, and experimental validation of a high-speed supercavitating vehicle // IEEE Journal of Oceanic Engineering. — 2015. — Vol. 40, no. 2. — P. 362–373.

[31] McNitt A., Dzielski J., Stinebring D. Experimental validation of planing models for a supercavitating vehicle // UDT Pacific 2006 Conference Proceedings. — San Diego, CA. — 2006. — The Applied Research Laboratory of Pennsylvania State University.

[32] Artificial cavitation. Physics and calculations : RTO-AVT/VKI Special Course on Supercavitating Flows / VKI ; executor: Semenenko V. N. — Brussels : 2001.

[33] Буйвол В. Н. Тонкие каверны в течениях с возмущениями. — Киев : Наукова думка, 1980. — 296 с.

[34] Эпштейн Л. А. Методы теории размерностей и подобия в задачах гидромеханики судов. — Ленинград : Судостроение, 1970. — 206 с.

[35] Логвинович Г. В., Серебряков В. В. О методах расчета формы тонких осесимметричных каверн // Гидромеханика. — 1975. — Т. 32, № 47–54.

[36] Логвинович Г. В. Вопросы теории тонких осесимметричных каверн // Труды ЦАГИ. — 1976. — № 1797. — С. 3–17.

[37] Парышев Е. В. Теоретическое исследование устойчивости и пульсаций осесимметричных каверн // Труды ЦАГИ. — 1978. — № 1907. — С. 17–40.

[38] Schlichting H. Boundary layer theory. — Oxford : Pergamon Press, 1956. — 535 p.

[39] Steady two-dimensional cavity flows about slender bodies : Rep. : 834 / David Taylor Model Basin ; executor: Tulin M. P. : 1953.

[40] Єфремов І. І. Лінеаризована теорія кавітаційного обтікання. — Київ : Інститут гідромеханіки АН УРСР, 1974.

[41] Искусственная кавитация / Егоров И. Т., Садовников Ю. М., Исаев И. И. и Басин М. А. — Ленинград : Судостроение, 1971. — 280 с.

[42] Resistance test. high speed marine vehicles. Testing and extrapolation methods : Recommended Procedures and Guidelines : 7.5-02 -05-01 / ITTC : 2008.

[43] Fresh water seawater properties : Recommended Procedures and Guidelines : 7.5-02-01-03 / ITTC : 2011.

[44] Кочин В. А., Мороз В. В. Автоматизированная система сбора и обработки данных скоростного опытого бассейна // Современные технологии автоматизации. — 2009. — № 3. — С. 48–50.

[45] Water entry and the cavity-running behavior of missiles : Rep. : 75-2 / Naval Surface Weapons Center, White Oak Laboratory ; executor: May A. — Silver Spring, MD : 1975.

[46] Серебряков В. В. Сопротивление осесимметричных кавитаторов при малых числах кавитации // Прикладна гідромеханіка. — 2014. — Т. 16(88), № 4. — С. 54–65.

В. В. Мороз, В. О. Кочін, В. М. Семененко, Бу-Ген Пайк

Теоретичне й експериментальне дослідження динаміки суперкавітаційних апаратів з конічними кавітаторами

Розглянуто математичну модель динаміки суперкавітаційного підводного апарату на основі повної системи рівнянь руху витягнутого твердого тіла з шістьма ступенями вільності. Виходячи з принципу Г. В. Логвиновича незалежності розширення перерізів каверни, для розрахунку суперкавітаційної течії використовувалась наближена математична модель «тонкої» порожнини. Гідродинамічні сили, що діють на різні елементи конструкції підводного апарату, були оцінені з використанням апроксимаційних залежностей, отриманих як з експериментальних, так і теоретичних розв'язків. Розроблену математичну модель динаміки суперкавітаційного апарату верифіковано шляхом порівняння розрахункових параметрів із отриманими під час буксирних випробувань моделі суперкавітаційного підводного апарату в швидкісному експериментальному лотку Інституту гідромеханіки НАН України. Основну увагу приділено динаміці суперкавітаційних моделей з конусними кавітаторами. На підставі результатів експерименту запропоновано нову апроксимаційну формулу для підйому на похилих конусних кавітаторах. Проведено порівняння розрахункової та експериментальної форми стаціонарної та нестаціонарної каверн за похилими конусними кавітаторами. Перевірку математичної моделі «в цілому» було проведено шляхом порівняння розрахованих кінематичних параметрів з отриманими при буксирних випробуваннях рухомої суперкавітаційної моделі з одним ступенем вільності по тангажу. При випробуваннях організовувалися різні режими руху суперкавітаційної моделі: ковзання по нижній стінці каверни; ковзання по верхній стінці каверни; рух ластами без торкання корпусом моделі стінок каверни; коливальний рух між верхньою і нижньою стінками каверни. Проведено порівняння експериментальних та розрахункових кінематичних характеристик суперкавітаційної моделі. Їх достатньо хороший якісний і кількісний збіг показує, що розроблена математична модель адекватно прогнозує динамічну поведінку підводного суперкавітуючого апарату.

КЛЮЧОВІ СЛОВА: динаміка суперкавітуючого апарату, конусний кавітатор, математична модель, комп'ютерне моделювання, експериментальна перевірка